Half-duplex Two-way Relaying for Wireless Sensor Networks with Adaptive Coding Rate: A Performance Optimization Framework

The-Anh Ngo[1], Viet-Thanh Le[2], Thien P. Nguyen[2], and Duy-Hung Ha[2]

[1] *University of Transport and Communications, Ho Chi Minh City, Vietnam,*
[2] *Ton Duc Thang University, Ho Chi Minh City, Vietnam*

https://doi.org/10.26636/jtit.2025.4.2314

Abstract — In this paper, a novel framework to enhance the reliability of wireless sensor networks (WSNs) by addressing the high probability of outage (OP) resulting from limited energy resources and unreliable channels. The framework integrates three techniques: half-duplex two-way relaying (HD-TWR), digital network coding (DNC), and rateless codes. Although these techniques have been extensively studied in isolation, a comprehensive analysis of their joint performance is provided as the main contribution. The proposed scheme leverages the energy efficiency of HD-TWR, the transmission reduction capability of DNC, and the retransmission-free resilience of rateless codes. Simulation results show that the integrated framework significantly reduces OP, offering a robust and practical solution to enhance the reliability enhancement. Furthermore, the impact of optimal relay node placement is investigated through parameter adjustments in the simulation stage to maximize performance gains.

Keywords — digital network coding, half-duplex two-way relaying, outage probability, rateless codes, relay placement, wireless sensor networks

1. Introduction

In the past decade, wireless sensor networks (WSNs) have become a foundational technology for real-time monitoring and data acquisition in a wide range of applications, from environmental surveillance to industrial automation. Comprised of numerous low-power sensor nodes, WSNs are crucial enablers of the Internet of Things (IoT) [1]–[3]. However, the performance of these networks is limited by their resource-constrained environments, energy resources, inherent unreliability, and security vulnerabilities of wireless channels. These limitations collectively lead to critical performance issues, particularly high outage probability (OP) and loss of secrecy, which compromise network reliability and data confidentiality. Therefore, developing robust, energy efficient, and secure communication protocols is a paramount challenge in WSNs [4]–[6].

To address the mentioned limitations, various advanced communication strategies have been investigated. First, node deployment techniques to enhance network coverage and data security have been studied in [3], [5], [7], [8]. Next, cooperative relaying has emerged as a key solution for improving network performance, such as throughput and outage probability as well as network lifetime, end-to-end delay, and secrecy [9]–[12]. While full-duplex relaying offers significant gains in spectral efficiency, its practical implementation is often hindered by the complex and power-intensive problem of mitigating residual self-interference cancelation.

On the contrary, half-duplex (HD) operation, which avoids simultaneous transmission and reception, inherently bypasses this issue [13]–[16]. HD relaying is simpler and more energy-efficient than their full-duplex counterparts as they only transmit or receive at any given time, making them a suitable choice for WSNs [16]. Moreover, a combination of HD and two-way relaying (TWR) can be useful to improve network performance [17], [18].

On a more fundamental level, digital network coding (DNC) is a powerful principle to enhance network efficiency. Rather than simply forwarding packets, DNC allows an intermediate node to combine data from multiple incoming streams before transmission (e.g., using an XOR operation) [19]. This technique significantly reduces the number of transmissions required to exchange information, thereby improving both network throughput and spectral efficiency.

To further bolster network reliability against channel impairments, rateless coding offers a decent solution. Unlike conventional fixed-rate codes that require a reliable channel to be effective, rateless codes (RC) allow a source to generate an infinite stream of encoded symbols, ensuring that a receiver can successfully decode the original message as soon as a sufficient number of symbols are collected. This property makes RC highly suitable for dynamic and unpredictable as well as unsecured wireless environments [20]–[24].

Although significant progress has been achieved, the aforementioned studies have been carried out independently. Building on these advancements, this work proposes a novel communication framework that integrates HD-TWR, DNC, and RC strategies. The core objective of this research is to signifi-

cantly minimize OP by also considering the optimal placement of the relay node. We develop a comprehensive analytical framework to model system outage performance for various network scenarios.

The key contributions of this work are the integration of rateless coding with a practical DNC-based HD-TWR scheme and a simulation-based demonstration of how the position of the relay affects system performance.

The remainder of this paper is organized as follows: Section 2 reviews related work. Section 3 details the system model. Section 4 provides the outage performance analysis. Section 5 presents the simulation results and discussions. Finally, Section 6 concludes the article and outlines potential future work.

2. Related Works

Research on enhancing the performance of wireless communication networks, particularly wireless sensor networks (WSNs), has evolved along several key directions, most notably in the areas of relaying strategies, advanced coding schemes, and network optimization. This section reviews the most pertinent literature related to wireless communications and WSNs, emphasizing the contributions and limitations of existing studies that motivate the integrated approach advanced in this paper.

2.1. Cooperative Relaying and HD-TWR

The fundamental principles of half-duplex relaying have been studied in prior work [15], [16], [25]–[27], which demonstrate that separating transmission and reception into orthogonal slots mitigates self-interference and simplifies transceiver design. In the simplest HD model, a relay node (RN) facilitates communication between two source nodes, requiring three time slots for the corresponding transmission phases, since the RN cannot transmit and receive simultaneously. These studies suggest that HD relaying can improve energy efficiency, transmission rate, probability of outage, and reliability in resource-constrained wireless communication systems. However, they remain largely limited to basic performance evaluations without addressing broader efficiency considerations.

Building on this foundation, subsequent research on half-duplex two-way relaying (HD-TWR) [17], [18], [28] investigates bidirectional communication, thereby reducing latency and improving spectral efficiency compared to conventional one-way relaying. Although these studies report notable performance gains, they also reveal persistent limitations. The half-duplex constraint inherently reduces throughput compared to full-duplex systems, and the effectiveness of HD-TWR is further challenged by channel estimation errors, synchronization difficulties, and relay processing overhead.

Furthermore, none of the existing HD-TWR works mentioned above has explored the integration of advanced coding techniques such as rateless codes and digital network coding, which holds significant promise for enhancing adaptability, reliability, and overall network performance. This research gap indicates that current HD and HD-TWR frameworks are insufficient to provide scalable, secure, and energy-efficient solutions for WSNs and next-generation wireless networks, thus motivating integrated approaches that jointly exploit relaying, coding, and network optimization to achieve practical improvements in efficiency, robustness, scalability, and secrecy performance.

2.2. Digital Network Coding and Rateless Codes

Digital network coding, typically implemented through XOR operations at the relay, reduces the number of transmission phases by combining packets from different sources, thus improving throughput, spectral efficiency, and latency in wireless communication systems [18], [19]. Despite these benefits, DNC remains sensitive to synchronization errors, imperfect channel estimation, and error propagation, which limit its robustness in practical scenarios.

Rateless codes extend the principle to generate an unlimited stream of coded packets, allowing receivers to decode once a sufficient number of symbols has been collected [29]. In general, RCs encompass a broad class of coding schemes such as Luby transform (LT), raptor, and random linear network coding (RLNC). In RLNC, each encoded packet is a random linear combination of source packets over a finite field.

In this paper, we consider a generic RC model without specifying the exact encoding structure, focusing on OP performance rather than decoding complexity. This general formulation allows the proposed framework to capture the performance behavior of various RC schemes without being restricted to a specific encoding algorithm. This rateless property not only enhances adaptability, reliability, and outage performance in time-varying channels but also provides inherent physical layer security (PLS), since eavesdroppers who do not accumulate enough packets cannot reconstruct the original data.

Recent studies confirm that CR can improve secrecy capacity, increase secrecy throughput, and reduce the probability of secrecy outages by exploiting channel asymmetry [18], [20], [22], [24], [30]. However, RC also suffers from decoding complexity, signaling overhead, and delay, particularly in large-scale networks. Although the integration of RC and DNC in full-duplex two-way relaying (FD-TWR) has been investigated [18], OP analysis has not been addressed. This gap provides the main motivation for the present work.

2.3. Relay Node Placement

Node deployment and relay selection are fundamental design aspects in cooperative wireless networks, as they directly influence coverage, reliability, and spectral efficiency [3], [5], [7], [8], [31]. However, none of the existing studies have evaluated network performance in terms of OP for HD-TWR systems that employ integrated RC and DNC. Given that OP is a critical metric for assessing link reliability under realistic channel conditions, its absence in previous research represents a significant gap. Therefore, it is essential

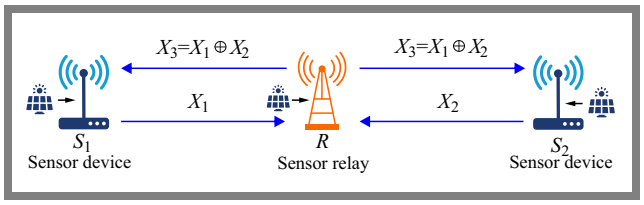

Fig. 1. The HD-TWR model using DNC and RC.

to conduct a comprehensive study on OP improvement of OP in HD-TWR systems with RC-DNC, providing deeper insight into system performance and reliability.

In summary, although HD-TWR has been widely studied, existing works have not incorporated advanced coding techniques such as RC and DNC, which could jointly improve adaptability, efficiency, and secrecy performance. On the contrary, research on RC and DNC has primarily addressed throughput, spectral efficiency, or physical layer security, but has not considered their integration into HD-TWR frameworks. Additionally, these studies typically overlook critical system-level aspects such as relay node deployment and placement optimization, which have a direct impact on coverage, reliability and OP. This gap indicates that current approaches remain insufficient to achieve robust and scalable performance in realistic network scenarios.

Motivated by these limitations, this article investigates the joint application of RC and DNC in HD-TWR systems, with a particular focus on evaluating and improving OP under different operating conditions. Additionally, we analyze the effect of relay node placement through simulation-based parameter adjustment, providing insights into optimal deployment strategies for improved system performance.

The relay node is assumed to be located along the line between S_1 and S_2. Let x_R denote its normalized position, where $x_R = 0$ and $x_R = 1$ correspond to the locations of S_1 and S_2, respectively. The effect of the placement of the relay on the outage probability is analyzed by varying x_R in the range $\{0,1\}$.

3. System Model

The system model using the HD-TWR relaying strategy combined with DNC-RC techniques (denoted as SM3P) is shown in Fig. 1. Two nodes, S_1 and S_2, exchange data via a relay R. Using RC, S_1 and S_2 split the original message into equal-size packets and XOR one or multiple selected packets to produce encoded packets.

Figure 1 depicts the process of exchanging encoded packets between S_1 and S_2, where $x_1(x_2)$ represents an encoded packet of $S_1(S_2)$ that needs to be sent to $S_2(S_1)$. Specifically, in the first phase, S_1 transmits x_1 to R, and in the subsequent phase, S_2 transmits x_2 to R. If R successfully decodes both x_1 and x_2, it performs the XOR operation as follows: $x_3 = x_1 \oplus x_2$. Subsequently, R transmits x_3 to both S_1 and S_2. Upon successfully decoding x_3, $S_1(S_2)$ can retrieve the desired $x_2(x_1)$ using the operation: $x_1 \oplus x_3 = x_2$ $(x_2 \oplus x_3 = x_1)$.

To successfully recover each other's original information, S_1 and S_2 are assumed to receive at least H packets without errors. Moreover, due to latency constraints, S_1 and S_2 can attempt to exchange their information packets x_1 and x_2 through at most Q transmission rounds, where $Q \geqslant H$. The transmission is considered successful if at least H out of Q encoded packets are correctly received and decoded. Indeed, upon the completion of data transmission, if $S_1(S_2)$ has not received the required number of packets, it will fail to recover the original information of $S_2(S_1)$, leading to an outage. It is also assumed that devices S_1, S_2, and R are equipped with a single antenna and that all transmission channels experience Rayleigh fading.

Additionally, this paper considers block fading channels, where the channel between two nodes remains constant within a phase but changes independently in subsequent transmission phases.

Considering data transmission in phase 1, the channel capacity between S_1 and R is given by:

$$C_{S_1 \to R} = \frac{1}{3} \log_2 \left(1 + \frac{P_1 \gamma_{S_1 \to R}}{\sigma_0^2} \right), \tag{1}$$

where, $\frac{1}{3}$ indicates that the transmission of each encoded packet occurs over three orthogonal time slots. The transmit power of S_1 is denoted as P_1, while $\gamma_{S_1 \to R}$ represents the channel gain between the nodes in phase 1. Additionally, σ_0^2 denotes the power of the additive white Gaussian noise (AWGN) at R (as well as at other receiving devices).

If $C_{S_1 \to R} \geqslant C_{th}$, we assume that R can successfully decode x_1, where C_{th} is a predefined threshold. Conversely, if $C_{S_1 \to R} < C_{th}$, x_1 cannot be decoded at R. Similarly, the channel capacity between S_2 and R is given by:

$$C_{S_2 \to R} = \frac{1}{3} \log_2 \left(1 + \frac{P_2 \gamma_{S_2 \to R}}{\sigma_0^2} \right), \tag{2}$$

where P_2 is the transmit power of S_2, and $\gamma_{S_2 \to R}$ represents the channel gain between the nodes in phase 2.

Similar to x_1, if $C_{S_2 \to R} \geqslant C_{th}$, the packet x_2 is successfully decoded at node R. Otherwise, node R fails to decode x_2.

Consequently, there exist four distinct cases regarding the decoding capability of node R for x_1 and x_2:

- **Case 1:** Neither x_1 nor x_2 is successfully decoded.
  In this scenario, $C_{S_1 \to R} < C_{th}$ and $C_{S_2 \to R} < C_{th}$. As a result, node R cannot transmit any encoded packet in phase 3 since both x_1 and x_2 are erroneously decoded (i.e., sources S_1 and S_2 do not receive any encoded packet).
- **Case 2:** x_1 is successfully decoded, while x_2 is not.
  In this case, $C_{S_1 \to R} \geqslant C_{th}$ and $C_{S_2 \to R} < C_{th}$. Consequently, R will transmit x_1 to S_2 in phase 3, and the achievable channel capacity is:

$$C_{R \to S_2} = \frac{1}{3} \log_2 \left(1 + \frac{P_3 \gamma_{R \to S_2}}{\sigma_0^2} \right), \tag{3}$$

  where P_3 is the transmit power of R, and $\gamma_{R \to S_2}$ denotes the channel gain between R and S_2.
- **Case 3:** x_2 is successfully decoded, while x_1 is not.
  In this scenario, $C_{S_1 \to R} < C_{th}$ and $C_{S_2 \to R} \geqslant C_{th}$. Thus,

R will forward x_2 to S_1 in phase 3, and the achievable channel capacity is:

$$C_{R\to S_1} = \frac{1}{3}\log_2\left(1+\frac{P_3\gamma_{R\to S_1}}{\sigma_0^2}\right), \tag{4}$$

where $\gamma_{R\to S_1}$ represents the channel gain between R and S_1.

- **Case 4:** Both x_1 and x_2 are successfully decoded. This case has been described earlier, where $C_{S_1\to R} \geqslant C_{th}$ and $C_{S_2\to R} \geqslant C_{th}$. In this situation, R will transmit x_3 to both S_1 and S_2, and the corresponding channel capacities are given by:

$$\begin{aligned} C_{R\to S_1} &= \frac{1}{3}\log_2\left(1+\frac{P_3\gamma_{R\to S_1}}{\sigma_0^2}\right), \\ C_{R\to S_2} &= \frac{1}{3}\log_2\left(1+\frac{P_3\gamma_{R\to S_2}}{\sigma_0^2}\right). \end{aligned} \tag{5}$$

4. Outage Probability Analysis

In this section, section a mathematical analysis of the outage probability at S_1 and S_2, which represents the probability that $S_1(S_2)$ fails to receive H encoded packets from $S_2(S_1)$. Given that the transmission channels experience Rayleigh fading, the channel gain between the transmitting node A and the receiving node B, where $A, B \in \{S_1, S_2, R\}$, follows the distributions:

$$\begin{aligned} F_{\gamma_{A\to B}}(x) &= 1-\exp(-\lambda_{A,B}x), \\ f_{\gamma_{A\to B}}(x) &= \lambda_{A,B}\exp(-\lambda_{A,B}x), \end{aligned} \tag{6}$$

where $F_{\gamma_{A\to B}}(x)$ and $f_{\gamma_{A\to B}}(x)$ denote the cumulative distribution function (CDF) and probability density function (PDF) of the channel gain $\gamma_{A\to B}$, respectively. Here, $\lambda_{A,B} = (d_{A,B})^\beta$ [22], with $d_{A,B}$ representing the distance between A and B, and β being the path loss exponent, where λ is the exponential parameter. In Rayleigh fading, the instantaneous SNR $\gamma = P|h|^2/N_0$ follows an exponential distribution with mean λ^{-1}. Therefore, λ corresponds to the inverse of the average SNR parameter.

A packet x_2 fails to reach S_1 if at least one of the two links, $S_2 \to R$ or $R \to S_1$, does not meet the required quality, i.e., $C_{S_2\to R} < C_{th}$ or $C_{R\to S_1} < C_{th}$. Consequently, the probability that an encoded packet from S_2 cannot be successfully transmitted to S_1 is expressed as:

$$\begin{aligned} \theta_{S_1} &= \Pr(C_{S_2\to R} \geqslant C_{th} \cup C_{R\to S_1} \geqslant C_{th}) \\ &= 1-\Pr(C_{S_2\to R} > C_{th} \cap C_{R\to S_1} > C_{th}) \\ &= 1-\Pr(C_{S_2\to R} > C_{th})\Pr(C_{R\to S_1} > C_{th}). \end{aligned} \tag{7}$$

Substituting the results from Eqs. (2) and (4) into Eq. (7), we obtain:

$$\begin{aligned} \theta_{S_1} &= 1-\Pr(\gamma_{S_2\to R} > \rho_2)\Pr(\gamma_{R\to S_1} > \rho_3) \\ &= 1-\Big(1-F_{\gamma_{S_2\to R}}(\rho_2)\Big)\Big(1-F_{\gamma_{R\to S_1}}(\rho_3)\Big), \end{aligned} \tag{8}$$

where:

$$\rho_2 = \frac{\left(2^{3C_{th}}-1\right)\sigma_0^2}{P_2}, \quad \rho_3 = \frac{\left(2^{3C_{th}}-1\right)\sigma_0^2}{P_3}. \tag{9}$$

By substituting the CDF functions from Eq. (6) into Eq. (8), we obtain:

$$\theta_{S_1} = 1-\exp\left(-\lambda_{S_2,R}\rho_2\right)\exp\left(-\lambda_{S_1,R}\rho_3\right). \tag{10}$$

Similarly, the probability that an encoded packet from S_1 fails to be successfully transmitted to S_2 is given by:

$$\begin{aligned} \theta_{S_2} &= \Pr\left(C_{S_1\to R} \leqslant C_{th} \cup C_{R\to S_2} \geqslant C_{th}\right) \\ &= 1-\left(1-F_{\gamma_{S_1\to R}}(\rho_1)\right)\left(1-F_{\gamma_{R\to S_1}}(\rho_3)\right) \\ &= 1-\exp\left(-\lambda_{S_1,R}\rho_1\right)\exp\left(-\lambda_{S_1,R}\rho_3\right), \end{aligned} \tag{11}$$

where $\rho_1 = \dfrac{\left(2^{3C_{th}}-1\right)\sigma_0^2}{P_1}$.

After the packet exchange process, let n_1 and n_2 denote the number of packets successfully received at S_1 and S_2, respectively. Considering S_2, the original information from S_1 can be successfully reconstructed if $n_2 \geqslant H$. If $n_2 < H$, then S_2 fails to reconstruct the information, resulting in an outage. Using Eq. (11), the OP at S_2 is derived as:

$$\begin{aligned} OP_{S_2}^{SM3P} &= \sum_{n_2=0}^{H-1} C_Q^{n_2}\left(1-\theta_{S_2}\right)^{n_2}\left(\theta_{S_2}\right)^{Q-n_2} \\ &= \sum_{n_2=0}^{H-1} C_Q^{n_2}\exp\left(-n_2\lambda_{S_1,R}\rho_1 - n_2\lambda_{S_1,R}\rho_3\right) \\ &\quad\times\left[1-\exp\left(-\lambda_{S_1,R}\rho_1-\lambda_{S_1,R}\rho_3\right)\right]^{Q-n_2}, \end{aligned} \tag{12}$$

where $C_Q^{n_2} = \dfrac{Q!}{n_2!\,(Q-n_2)!}$ denotes the binomial coefficient.

Note that any subset of H correctly received packets out of Q total attempts is sufficient for successful decoding.

Similarly, the outage probability at the source S_1 is given by the following exact closed-form expression:

$$\begin{aligned} OP_{S_1}^{SM3P} &= \sum_{n_1=0}^{H-1} C_Q^{n_1}\left(1-\theta_{S_1}\right)^{n_1}\left(\theta_{S_1}\right)^{Q-n_1} \\ &= \sum_{n_1=0}^{H-1} C_Q^{n_1}\exp\left(-n_1\lambda_{S_2,R}\rho_2 - n_1\lambda_{S_1,R}\rho_3\right) \\ &\quad\times\left[1-\exp\left(-\lambda_{S_2,R}\rho_1-\lambda_{S_1,R}\rho_3\right)\right]^{Q-n_1}. \end{aligned} \tag{13}$$

Next, the conventional four-phase HD-TWR model, referred to as SM4P will be analysed. In this model, the first two transmission phases are used to transmit x_1 from S_1 through R to S_2, while the remaining two phases are used to transmit x_2 from S_2 through R to S_1. Due to the four-phase transmission scheme, the channel capacity of the links is determined as follows:

$$\begin{aligned} C_{S_1\to R}^* &= \frac{1}{4}\log_2\left(1+\frac{P_1\gamma_{S_1\to R}}{\sigma_0^2}\right), \\ C_{R\to S_2}^* &= \frac{1}{4}\log_2\left(1+\frac{P_3\gamma_{R\to S_2}}{\sigma_0^2}\right), \\ C_{S_2\to R}^* &= \frac{1}{4}\log_2\left(1+\frac{P_2\gamma_{S_2\to R}}{\sigma_0^2}\right), \\ C_{R\to S_1}^* &= \frac{1}{4}\log_2\left(1+\frac{P_3\gamma_{R\to S_1}}{\sigma_0^2}\right). \end{aligned} \tag{14}$$

Using the same analytical approach as in SM3P, the probabilities that S_1 and S_2 fail to achieve a single encoded packet are given as follows:

$$\begin{aligned}\theta^*_{S_1} &= \Pr\left(C^*_{S_2\to R} \leqslant C_{th} \cup C^*_{R\to S_1} \leqslant C_{th}\right)\\ &= 1-\exp\left(-\lambda_{S_2,R}\theta_2\right)\exp\left(-\lambda_{S_1,R}\theta_3\right),\\ \theta^*_{S_2} &= \Pr\left(C^*_{S_1\to R} \leqslant C_{th} \cup C^*_{R\to S_2} \leqslant C_{th}\right)\\ &= 1-\exp\left(-\lambda_{S_1,R}\theta_2\right)\exp\left(-\lambda_{S_1,R}\theta_3\right),\end{aligned} \tag{15}$$

where:

$$\begin{aligned}\theta_1 &= \frac{(2^{4C_{th}}-1)\sigma_0^2}{P_1},\\ \theta_2 &= \frac{(2^{4C_{th}}-1)\sigma_0^2}{P_2},\\ \theta_3 &= \frac{(2^{4C_{th}}-1)\sigma_0^2}{P_3}.\end{aligned} \tag{16}$$

Subsequently, the OP at S_1 and S_2 in SM4P is respectively given by the following exact closed-form expressions:

$$\begin{aligned}OP_{S_1}^{SM4P} &= \sum_{n_1=0}^{H-1} C_Q^{n_1}\left(1-\theta^*_{S_1}\right)^{n_1}\left(\theta^*_{S_1}\right)^{Q-n_1}\\ &= \sum_{n_1=0}^{H-1} C_Q^{n_1}\exp\left(-n_1\lambda_{S_2,R}\theta_2 - n_1\lambda_{S_1,R}\theta_3\right)\\ &\quad\times\left[1-\exp\left(-\lambda_{S_2,R}\theta_2-\lambda_{S_1,R}\theta_3\right)\right]^{Q-n_1},\end{aligned} \tag{17}$$

$$\begin{aligned}OP_{S_2}^{SM4P} &= \sum_{n_2=0}^{H-1} C_Q^{n_2}\left(1-\theta^*_{S_2}\right)^{n_2}\left(\theta^*_{S_2}\right)^{Q-n_2}\\ &= \sum_{n_2=0}^{H-1} C_Q^{n_2}\exp\left(-n_2\lambda_{S_1,R}\theta_1 - n_2\lambda_{S_1,R}\theta_3\right)\\ &\quad\times\left[1-\exp\left(-\lambda_{S_1,R}\theta_1-\lambda_{S_1,R}\theta_3\right)\right]^{Q-n_2},\end{aligned} \tag{18}$$

Before proceeding to Section 5, we consider the power allocation problem for S_1, S_2, and R, formulated as follows:

$$P_1+P_2+P_3 = P\,. \tag{19}$$

Equation (19) implies that the total transmit power of all nodes is constrained to P, and we need to allocate P_1, P_2, and P_3 to achieve optimal OP performance.

First, considering that S_1 and S_2 are typically identical devices, we assume equal transmit power for both, i.e., $P_1 = P_2 = P_S$. Consequently, Eq. (19) simplifies to $2P_S+P_3 = P$. Therefore, if we set $P_S = \mu P$, the transmit power of R is given by $P_R = P_3 = (1-2\mu)P$, where μ $(0<\mu<0.5)$ is a predetermined coefficient.

5. Simulation Results and Discussions

In this section, we perform Monte Carlo simulations to verify the derived OP formulas, such as (12), (13), (17), and (18).

Consider the axis O_x, where S_1, S_2, and R have coordinates $S_1(0)$, $S_2(1)$, and $R(x_R)$, respectively, with $0<x_R<1$. Given these positions, the distance between S_1 and S_2 is fixed at 1, while R moves between S_1 and S_2. The distances between R and the sources are expressed as $d_{S_1,R} = x_R$ and $d_{S_2,R} = 1-x_R$.

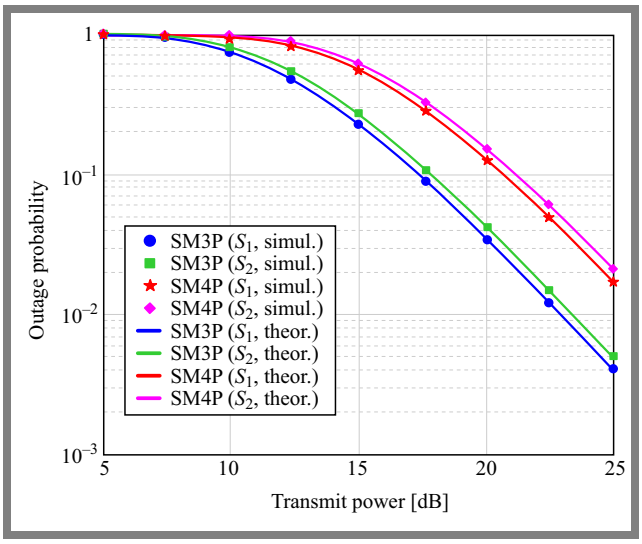

Fig. 2. Outage probability vs. transmit power (in decibels) with $H=4$, $Q=5$, $x_R=0.35$, and $\mu=0.35$.

To focus on investigating the impact of key parameters, we fix the following system parameters: noise power $\sigma_0^2=1$, outage threshold $C_{th}=1$, and path-loss exponent $\beta=3$.

Figure 2 plots the OP of S_1 and S_2 in both SM3P and SM4P models versus P [dB]. In Fig. 2, the system parameters are set as $H=4$, $Q=5$, x_R=0.35, and μ=0.35. With μ=0.35, the transmit powers of the nodes are P_S=0.35P and P_R=0.3P. Figure 2 shows that the OP of both S_1 and S_2 decreases as P increases because higher P leads to higher P_S and P_R. We also observe that the OP of S_1 and S_2 in SM3P is lower than in SM4P since SM3P uses only three transmission phases.

Furthermore, in both SM3P and SM4P, the OP of S_1 is lower than that of S_2. This is because the transmit power of R is smaller than that of the source nodes ($P_S > P_R$). Additionally, R is farther from S_2, so the packet transmission from R to S_2 in phase 3 is less reliable than from R to S_1.

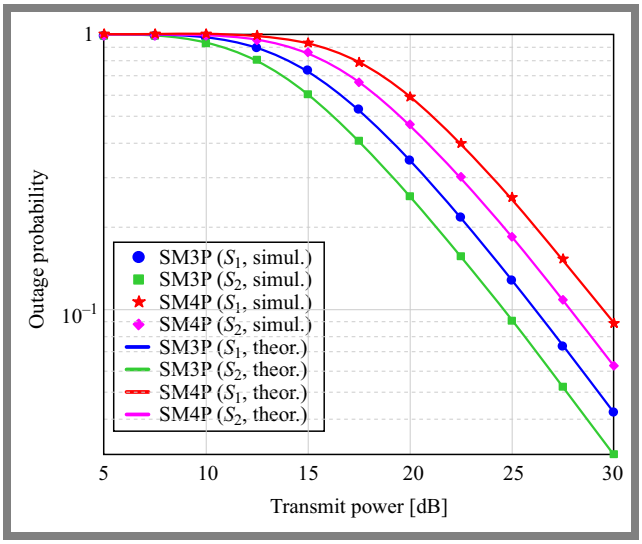

Fig. 3. Outage probability vs. transmit power (in decibels) with $H=5$, $Q=5$, $x_R=0.6$, and $\mu=0.4$

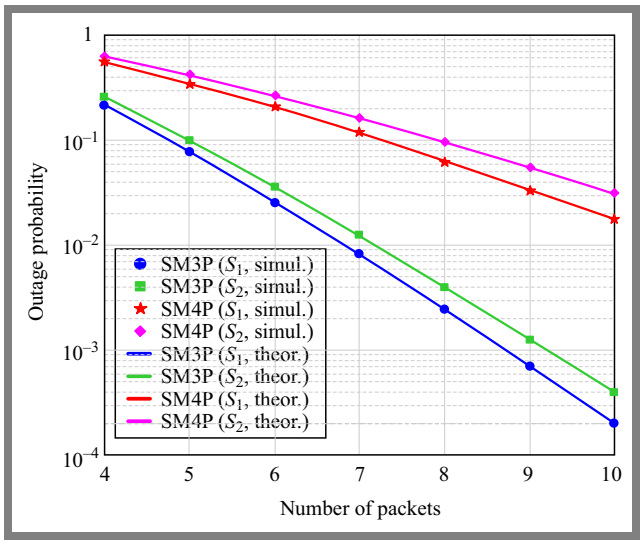

Fig. 4. Outage probability vs. number of packets with $P = 10$ dB, $H = 3$, $x_R = 0.55$, and $\mu = 0.3$.

The results in Fig. 2 also demonstrate excellent agreement between simulation and theory, validating the accuracy of the derived Eqs. (12), (13), (17), and (18) presented in Section 4.

Figure 3 illustrates the OP of S_1 and S_2 in SM3P and SM4P versus P [dB] with $H = 5$, $Q = 5$, $x_R = 0.6$, and $\mu = 0.4$. Similarly, SM3P achieves lower OP at both sources compared to SM4P. However, the OP at S_2 in both SM3P and SM4P is lower than at S_1. As explained for Fig. 2, this is because $P_S = 0.4P > P_R = 0.2P$, and R is closer to S_2 than to S_1, resulting in lower OP at S_2.

Figure 4 plots the OP at the sources as a function of the maximum number of retransmissions Q for $P = 10$ dB, $H = 3$, $x_R = 0.55$, and $\mu = 0.3$. As expected, the OP of all sources decreases as Q increases. Figure 4 also shows that the OP of SM3P and SM4P decreases faster with increasing Q. Moreover, the OP in SM3P decreases more rapidly than in SM4P. Thus, to enhance reliability (i.e., reduce OP) in SM3P and SM4P, we can increase Q. For example, in SM3P,

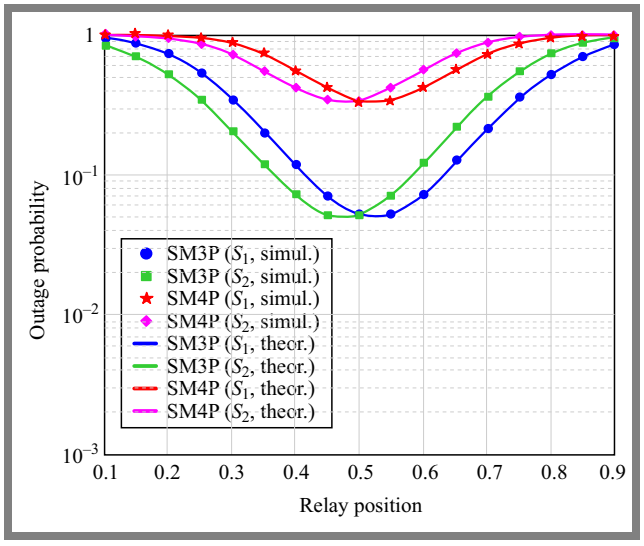

Fig. 5. Outage probability vs. relay position with $P = 10$ dB, $H = 4$, $Q = 7$, and $\mu = 0.3$.

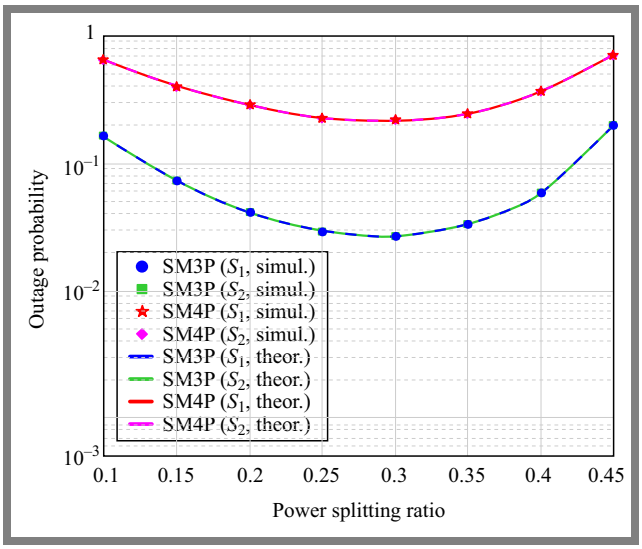

Fig. 6. Outage probability vs. power spliting ratio with $P = 10$ dB, $H = 3$, $Q = 6$, and $x_R = 0.5$.

$Q \geqslant 8$ is required to achieve OP < 0.001 at both sources. However, increasing Q also raises the network delay and energy consumption.

Figure 5 analyzes the impact of relay position x_R on system performance with $P = 10$ dB, $H = 4$, $Q = 7$, and $\mu = 0.3$. The results show that x_R significantly affects the OP at S_1 and S_2 in both SM3P and SM4P. Specifically, when $x_R < 0.5$, the OP at S_2 is lower than at S_1. Conversely, for $x_R > 0.5$, $OP_{S_1}^{SM3P} < OP_{S_2}^{SM3P}$ and $OP_{S_1}^{SM4P} < OP_{S_2}^{SM4P}$. At $x_R = 0.5$ (i.e., R is equidistant to both sources), the OP is balanced and minimized. Thus, placing R midway optimizes outage performance.

Figure 6 investigates the effect of μ on the OP in SM3P and SM4P with $P = 10$ dB, $H = 3$, $Q = 6$, and $x_R = 0.5$. Here, R is centered to ensure symmetric performance. The results reveal that μ critically influences the OP, and an optimal $\mu = \frac{1}{3}$ exists where $P_S = P_R = \frac{P}{3}$, minimizing the OP. Due to the complexity of the OP expressions, a rigorous proof of this optimum will be addressed in future work.

6. Conclusions

This paper proposed and analyzed a novel half-duplex two-way relaying (HD-TWR) framework incorporating digital network coding and rateless codes, with a focus on evaluating outage probability under different operating scenarios. The three-phase (SM3P) and four-phase (SM4P) schemes were investigated and closed-form OP expressions were derived, providing useful analytical tools for system optimization.

The simulation results demonstrate that the optimal relay position lies at the midpoint between the two sources, while the equal allocation of power between the nodes achieves the best outage performance.

Furthermore, increasing the maximum number of transmission attempts at the sources can enhance OP, though at the cost of higher latency and energy consumption. These findings

highlight the effectiveness of the proposed RC-DNC-based HD-TWR model in improving reliability and efficiency, while also providing practical guidelines for relay placement and resource allocation in cooperative wireless networks.

The proposed analysis is based on idealized assumptions with independent Rayleigh fading and equal retransmission probabilities. In practice, packet errors may be correlated, and the error rate may remain approximately constant within certain transmit power ranges due to hardware limitations.

However, the analytical trends derived here provide valuable qualitative information on how power allocation and relay placement affect system reliability. Despite these simplifications, the proposed model offers a tractable analytical foundation that can be extended to more realistic correlated-fading scenarios in future work.

For future work, the investigation of three-phase and four-phase HD-TWR models with advanced relay selection strategies, such as partial relay selection and optimal relay selection [7], [31], is suggested, as these approaches are expected to further enhance performance. Furthermore, the extension of the proposed framework to two-phase FD-TWR systems with RC-DNC integration will be considered to explore additional improvements in network performance.

Acknowledgments

This research is funded by University of Transport and Communications (UTC) under grant number T2025-PHII_DDT-001.

References

[1] M.N. Mowla *et al.*, "Internet of Things and Wireless Sensor Networks for Smart Agriculture Applications: A Survey", *IEEE Access*, vol. 11, pp. 145813–145852, 2023 (https://doi.org/10.1109/ACCESS.2023.3346299).

[2] M. Pundir *et al.*, "Dimensional-based Methods for Topological Management in Underwater Wireless Sensor Networks: A Comprehensive Survey", *IEEE Access*, vol. 13, pp. 67511–67530, 2025 (https://doi.org/10.1109/ACCESS.2025.3546978).

[3] M.F. Farsi *et al.*, "Deployment Techniques in Wireless Sensor Networks, Coverage and Connectivity: A Survey", *IEEE Access*, vol. 7, pp. 28940–28954, 2019 (https://doi.org/10.1109/ACCESS.2019.2902072).

[4] S. Najjar, M. David, W. Derigent, and A. Zouinkhi, "Dynamic Reconfiguration of Wireless Sensor Networks: A Survey", *Computer Networks*, vol. 262, art. no. 111176, 2025 (https://doi.org/10.1016/j.comnet.2025.111176).

[5] A. John, I.F.B. Isnin, S.H.H. Madni, and M. Faheem, "Intrusion Detection in Cluster-based Wireless Sensor Networks: Current Issues, Opportunities and Future Research Directions", *IET Wireless Sensor Systems*, vol. 14, pp. 293–332, 2024 (https://doi.org/10.1049/wss2.12100).

[6] K. Loukil, "Energy Saving Multi-relay Technique for Wireless Sensor Networks Based on Hw/Sw MPSoC System", *IEEE Access*, vol. 11, pp. 27919–27927, 2023 (https://doi.org/10.1109/ACCESS.2023.3259235).

[7] M.S. Ghahroudi, A. Shahrabi, S.M. Ghoreyshi, and F.A. Alfouzan, "Distributed Node Deployment Algorithms in Mobile Wireless Sensor Networks: Survey and Challenges", *ACM Transactions on Sensor Networks*, vol. 19, pp. 1–26, 2023 (https://doi.org/10.1145/3579034).

[8] M.M. Moslehi, "Exploring Coverage and Security Challenges in Wireless Sensor Networks: A Survey", *Computer Networks*, vol. 260, art. no. 111096, 2025 (https://doi.org/10.1016/j.comnet.2025.111096).

[9] H. Zhang *et al.*, "Secure Resource Allocation for OFDMA Two-way Relay Wireless Sensor Networks without and with Cooperative Jamming", *IEEE Transactions on Industrial Informatics*, vol. 12, pp. 1714–1725, 2016 (https://doi.org/10.1109/TII.2015.2489610).

[10] Z. Iqbal, K. Kim, and H.-N. Lee, "A Cooperative Wireless Sensor Network for Indoor Industrial Monitoring", *IEEE Transactions on Industrial Informatics*, vol. 13, pp. 482–491, 2017 (https://doi.org/10.1109/TII.2016.2613504).

[11] Aripriharta *et al.*, "A New Bio-inspired for Cooperative Data Transmission of IoT", *IEEE Access*, vol. 8, pp. 161884–161893, 2020 (https://doi.org/10.1109/ACCESS.2020.3021507).

[12] H.-H. Choi and K. Lee, "Cooperative Wireless Power Transfer for Lifetime Maximization in Wireless Multihop Networks", *IEEE Transactions on Vehicular Technology*, vol. 70, pp. 3984–3989, 2021 (https://doi.org/10.1109/TVT.2021.3068345).

[13] B. Hong and W. Choi, "Overcoming Half-duplex Loss in Multi-relay Networks: Multiple Relay Coded Cooperation for Optimal DMT", *IEEE Transactions on Communications*, vol. 63, pp. 66–78, 2015 (https://doi.org/10.1109/TCOMM.2014.2369054).

[14] C. Yao, H. Wu, and Z. Zhang, "A Novel Rateless Coded Protocol for Half-duplex Relaying Systems with Buffered Relay", *2018 IEEE 88th Vehicular Technology Conference (VTC-Fall)*, Chicago, USA, 2018 (https://doi.org/10.1109/VTCFall.2018.8690562).

[15] S. Panic, D.N.K. Jayakody, and S. Garg, "Self-energized Bidirectional Sensor Networks over Hoyt Fading Channels under Hardware Impairments", *2019 IEEE 90th Vehicular Technology Conference (VTC2019-Fall)*, Honolulu, USA, 2019 (https://doi.org/10.1109/VTCFall.2019.8891415).

[16] H. Shen *et al.*, "Is Full-duplex Relaying More Energy Efficient Than Half-duplex Relaying?", *IEEE Wireless Communications Letters*, vol. 8, pp. 841–844, 2019 (https://doi.org/10.1109/LWC.2019.2895649).

[17] F.-K. Gong, J.-K. Zhang, and J.-H. Ge, "Asymptotic SEP Analysis of Two-way Relaying Networks with Distributed Alamouti Codes", *IEEE Transactions on Vehicular Technology*, vol. 61, pp. 3777–3783, 2012 (https://doi.org/10.1109/TVT.2012.2210060).

[18] D. Jia *et al.*, "A Hybrid EF/DF Protocol with Rateless Coded Network Code for Two-way Relay Channels", *IEEE Transactions on Communications*, vol. 64, pp. 3133–3147, 2016 (https://doi.org/10.1109/TCOMM.2016.2583422).

[19] P. Popovski and H. Yomo, "Physical Network Coding in Two Way Wireless Relay Channels", *2007 IEEE International Conference on Communications*, Glasgow, UK, 2007 (https://doi.org/10.1109/ICC.2007.121).

[20] S. Jain and R. Bose, "Rateless Code-Aided Transmission Scheme to Achieve Secrecy in a Delay-Constraint Environment", *2019 IEEE International Conference on Advanced Networks and Telecommunications Systems (ANTS)*, Goa, India, 2019 (https://doi.org/10.1109/ANTS47819.2019.9118153).

[21] H. Wei and N. Deng, "On the Age of Information in Wireless Networks Using Rateless Codes", *IEEE Access*, vol. 8, pp. 173147–173157, 2020 (https://doi.org/10.1109/ACCESS.2020.3025431).

[22] D.-H. Ha *et al.*, "Security-reliability Trade-off Analysis for Rateless Codes-based Relaying Protocols Using NOMA, Cooperative Jamming and Partial Relay Selection", *IEEE Access*, vol. 9, pp. 131087–131108, 2021 (https://doi.org/10.1109/ACCESS.2021.3114343).

[23] H.-C. Lin, K.-H. Lin, and H.-Y. Wei, "Adaptive Age of Information Optimization in Rateless Coding-based Multicast-enabled Sensor Networks", *IEEE Journal of Selected Areas in Sensors*, vol. 1, pp. 73–92, 2024 (https://doi.org/10.1109/JSAS.2024.3407689).

[24] G. Huang *et al.*, "Improving Throughput in SWIPT-based Wireless Multirelay Networks with Relay Selection and Rateless Codes", *Digital Communications and Networks*, vol. 10, pp. 1131–1144, 2024 (https://doi.org/10.1016/j.dcan.2023.01.012).

[25] Y. Li *et al.*, "Relay Mode Selection and Power Allocation for Hybrid One-way/Two-way Half-duplex/Full-duplex Relaying", *IEEE Communications Letters*, vol. 19, pp. 1217–1220, 2015 (https://doi.org/10.1109/LCOMM.2015.2433260).

[26] J. Ma, C. Huang, and Q. Li, "Energy Efficiency of Full- and Half-duplex Decode-and-forward Relay Channels", *IEEE Internet of Things Journal*, vol. 9, pp. 9730–9748, 2022 (https://doi.org/10.1109/JIOT.2022.3143165).

[27] G. Srirutchataboon and S. Sugiura, "Secrecy Performance of Buffer-aided Hybrid Virtual Full-duplex and Half-duplex Relay Activation", *IEEE Open Journal of Vehicular Technology*, vol. 3, pp. 344–355, 2022 (https://doi.org/10.1109/OJVT.2022.3189612).

[28] L. Ong, "The Half-duplex Gaussian Two-way Relay Channel with Direct Links", *2015 IEEE International Symposium on Information Theory (ISIT)*, pp. 1891–1895, 2015 (https://doi.org/10.1109/ISIT.2015.7282784).

[29] A. Shokrollahi and M. Luby, "Raptor Codes", *Foundations and Trends in Communications and Information Theory*, vol. 6, pp. 213–322, 2011 (https://doi.org/10.1561/0100000060).

[30] P. Schulz *et al.*, "Efficient Reliable Wireless Communications through Raptor Codes and Rateless Codes with Feedback", *ICC 2022 - IEEE International Conference on Communications*, Seoul, South Korea, 2022 (https://doi.org/10.1109/ICC45855.2022.9838721).

[31] C. Huang *et al.*, "A Parallel Joint Optimized Relay Selection Protocol for Wake-up Radio Enabled WSNs", *Physical Communications*, vol. 47, art. no. 101320, 2021 (https://doi.org/10.1016/j.phycom.2021.101320).

The-Anh Ngo, Ph.D., Lecturer
Campus in Ho Chi Minh City
https://orcid.org/0009-0006-4976-1646
E-mail: anhnt_ph@utc.edu.vn
University of Transport and Communications, Ho Chi Minh City, Vietnam
https://utc2.edu.vn

Viet-Thanh Le, Lecturer
Faculty of Information Technology
https://orcid.org/0009-0000-8683-3158
E-mail: levietthanh@tdtu.edu.vn
Ton Duc Thang University, Ho Chi Minh City, Vietnam
https://tdtu.edu.vn

Thien P. Nguyen, Student
Faculty of Electrical and Electronics Engineering
https://orcid.org/0009-0008-0508-8167
E-mail: 42100891@student.tdtu.edu.vn
Ton Duc Thang University, Ho Chi Minh City, Vietnam
https://tdtu.edu.vn

Duy-Hung Ha, Ph.D., Lecturer
Wireless Communications Research Group
Faculty of Electrical and Electronics Engineering
https://orcid.org/0000-0001-6980-7273
E-mail: haduyhung@tdtu.edu.vn (Corresponding Author)
Ton Duc Thang University, Ho Chi Minh City, Vietnam
https://tdtu.edu.vn